Water balance in a neotropical forest catchment of southeastern Brazil

Carlos R. Mello[1*], Léo F. Ávila[1], Henry Lin[2,3,4], Marcela C.N.S. Terra[1], Nick A. Chappell[5]

[1]Soil and Water Engineering, Engineering Department, Federal University of Lavras, MG, Brazil, 37200-000, C.P. 3037, *Corresponding author. E-mail: crmello@deg.ufla.br

[2]Department of Ecosystem Science and Management, College Agricultural Science, Pennsylvania State University, State College, Pennsylvania, USA.

[3]State Key Laboratory of Loess and Quaternary Geology, Institute of Earth Environment, Chinese Academy of Sciences, Xi'an 710061, China

[4] State Key Laboratory of Eco-hydraulic Engineering in Arid Area, Xi'an University of Technology, Xi'an, 710048, China

[5]Lancaster Environmental Centre, Lancaster University, Lancaster, UK.

Abstract

Brazilian Atlantic Forest is recognized by the UNESCO as one of the most important biosphere reserve on the planet but is threatened by extinction. The objective of this study was to analyze the main components of the water balance in an Atlantic Forest (Neotropical Forest) catchment in Mantiqueira Range, Brazil, which is a Tropical Montane Cloud Forest. The main focuses were to analyze baseflow, evapotranspiration, soil moisture, and canopy rainfall interception to understand the hydrologic dynamics in this specially important montane forest. On average from the two studied hydrological years (2009/2010 and 2010/2011), evapotranspiration (ET), streamflow (SF), and water storage in the catchment in the end of hydrological year corresponded, respectively, to 50%, 34.8% and 15.2% of total gross precipitation (P). On average, baseflow

corresponded to 73.5% of SF. The estimated potential groundwater recharge during the wet seasons was 403.8 mm (21.7% of P observed in the wet season) and 710.5 mm (28.5% of P observed in the wet season), respectively, for 2009/2010 and 2010/2011 hydrological years, showing that the catchment is able to store groundwater to provide the maintenance of the streamflow during recession phase via baseflow as well as during drought periods. Therefore, the baseflow is important in mountainous catchments in the tropical regions to provide important ecological functions, mainly as freshwater reserve.

Keywords: Baseflow, Evapotranspiration, Tropical Montane Forest, Soil Moisture.

1 Introduction

The Brazilian Atlantic Forest has been recognized by the UNESCO as one of the most important biosphere reserve on the planet due to its endemic species and hydrological relevance. This ecosystem, which originally covered 100 million hectares (16% of the country's area), now covers less than 7 million hectares, mostly restricted to the mountainous regions of Southeastern Brazil (Galindo-Leal and Câmara 2003; Tabarelli et al. 2010). Due to human beings interventions, this kind of forest has been referred as Neotropical Forest remnant (Terra et al. 2017). Despite the environmental and ecological importance of the Neotropical Forests for the country, there are few studies detailing their hydrological functioning, especially regarding baseflow and its possible mechanisms and connections with other water balance components.

In tropical mountainous regions, the Neotropical Forest sites are known as Tropical Montane Cloud Forest (TMCF), and they are further classified in accordance

with its elevation and dominant species. TMCF sites have a complex interaction between forest canopy, weather, soils, and streamflow, which has led to controversies regarding its hydrological role in tropical regions, mainly in the context of the baseflow behavior. To overcome these controversies, some studies have been carried out towards detailing the water balance elements (i.e., streamflow, canopy rainfall interception, soil moisture, evapotranspiration. and their relationships) around the world, but they are scarce in the Brazilian Atlantic Forest. In this regard, the availability of datasets based on a continuous monitoring of streamflow, weather, soil moisture, and throughfall, covering both the ascension and recession of complete hydrological years, is imperative. One of these few studies was that done by Salemi et al. (2013), which was based on meteorological and streamflow monitoring and a few rain-gauges for throughfall measurement during a hydrological year. However, neither evapotranspiration nor soil moisture were studied.

In other sites around the world, Muñoz-Villers et al. (2012) studied the water balance components of two TMCF sites in the central region of Mexico. They stated that these catchments are laid on a bedrock and saprolite interfaces with good permeability, which indicates reasonable capacity for groundwater storage along with relevant interrelationship among the components of water balance. Fleischbein et al. (2005) and Fleischbein et al. (2006) also analyzed the water balance in a TMCF of the Equatorial Andes. They found that the canopy had a significant role in the protection of soils in terms of the overland flow generation, since the canopy reduces the impact of rainfall intensity over the ground, allowing greater opportunity for water infiltration. Wiekenkamp et al. (2016) studied the role of the soils in the hydrology of a TMCF site in Germany. They concluded that soils with mature native forest have shown high porosity and pores

interconnected that can generate preferential flows. These features lead to a higher infiltration capacity as well as greater natural streamflow regulation.

Muñoz-Villers et al. (2016) provided an important contribution to understanding the nature of the baseflow in a TMCF in the Central Mountainous region in Mexico. Based on hydrologic isotopic readings, they have proven that the baseflow can sustain the streamflow, even in a complex environment characterized by a steep topography and fractured bedrock. In the study in a TMCF site in Thailand by Hugenschmidt et al. (2014), they verified that the baseflow has presented greater predominance in relation to the overland flow. Caballero et al. (2012) studied a hydrological year in a TMCF in Central America and verified that the baseflow/streamflow ratio was approximately 80%, showing a greater predominance of the baseflow in the streamflow. All these studies demonstrated that the baseflow has been predominant in TMCF sites, especially if the native forests are preserved that can improve the soil's structure and permeability and thus favor soil-water infiltration and groundwater recharge (Ma et al. 2017; Wiekenkamp et al. 2016; Pinto et al. 2015).

Mantiqueira Range region is within the Atlantic Forest biome and was also recognized by UNESCO in 1992 as one of the most important biosphere reserve on the planet mainly because of its high-water yield capacity (Bruijnzeel et al. 2010). The region is one of the most important water sources for supplying the Metropolitan region of São Paulo (Coelho et al. 2015) and for feeding hydropower reservoirs located in the Grande river basin (Pinto et al. 2015). Its importance has been highlighted as strategic to mitigate harmful effects from persistent droughts, such as the one observed in Southeastern Brazil between 2014 and 2015 (Coelho et al. 2015). Thus, to understand the water balance in

TMCF catchments in Southeastern Brazil is critical for supporting management actions to reduce the impacts of scarce freshwater resource.

Thus, the objective of this study was to reveal the intrinsic relationship between hydrology, soil, and forest in a TMCF catchment of the Mantiqueira Range, focusing on the canopy rainfall interception, evapotranspiration, soil moisture, streamflow, and groundwater recharge using the framework of the water balance. More specifically, we sought to answer two relevant concerns that request a more comprehensive understanding of the water balance: (i) is the baseflow capable of supplying water continuously over the hydrological year or it is more prone to short-term fluctuations? And (ii) does the water balance in the catchment in this region end up in positive (i.e., with surplus)?

2 Study site

2.1 Location and forest measurements

The studied TMCF is referred to as an Atlantic Forest Micro-Catchment (AFMC), which is located within a larger experimental watershed called Lavrinha Creek Watershed (LCW) in Mantiqueira Range, Minas Gerais State, southeastern Brazil (Figure 1).

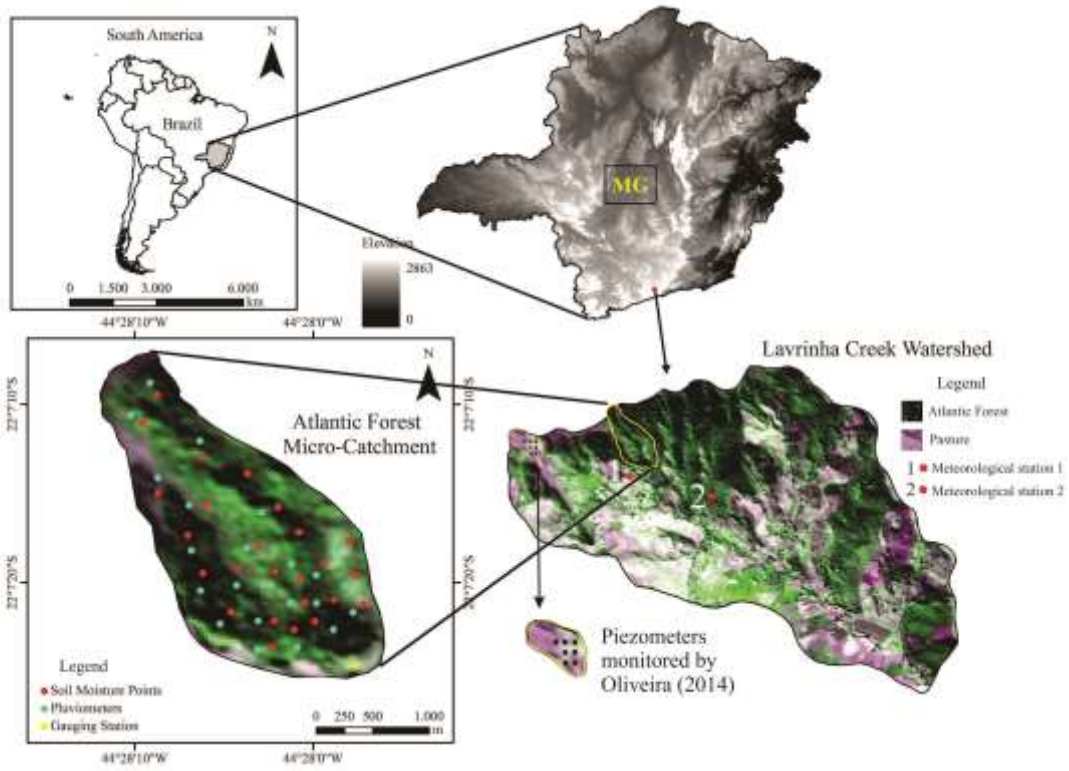

Figure 1. Geographical location and instrumentation used for monitoring water balance elements in the AFMC, Mantiqueira Range, Minas Gerais (MG) state, southeastern Brazil.

The AFMC encompasses 13.3 ha drainage area covered by a Dense Ombrophilous Forest, which is a typical physiognomy of the Atlantic Forest in the Mantiqueira Range (Oliveira Filho et al. 2006). Three forest inventories (2009, 2011, and 2012) were carried out in the AFMC by Terra et al. (2015a, b). During these surveys, all trees with diameter at breast height (1.3 m aboveground; DBH) larger than 5 cm had their DBH and height measured in 12 sampling plots of 300 m² size each randomly distributed in the AFMC. With these data, an equation adjusted by Scolforo et al. (2008), which is specific for this

121 forest physiognomy in Mantiqueira Range region, was used for estimating the existing
122 biomass in the AFMC. Therefore, the average density and basal area of the forest (2185.3
123 trees ha^{-1} and 24.5 m^2 ha^{-1}, respectively), the average canopy height (8.58 m ± 1.78), the
124 average Leaf Area Index (LAI) (4.05 m^2 m^{-2} ± 1.20 m^2 m^{-2}), and the carbon stock (39.06
125 t ha^{-1}) were calculated. The following tree species were identified by Terra et al. (2015a)
126 as most representative in the AFMC: *Lamanonia ternata* Vell., *Psychotria vellosiana*
127 Benth., *Myrsine umbellata* Mart., *Myrcia splendens* (Sw.) DC., *Clethra scabra* Pers.,
128 *Guapira opposita* (Vell.) Mart., *Miconia sellowiana* Naudin, *Inga sessilis* (Vell.) Mart.,
129 *Alchornea triplinervia* (Spreng.) Müll. Arg. and *Miconia cinerascens* Miq.

130

131 **2.2 Basic hydrologic and soil features at the AFMC**

132 Soil saturated hydraulic conductivity (Ks) at the AFMC was estimated by Pinto et
133 al. (2015) in their study about Inceptsols hydrological role in Mantiqueira Range region.
134 The procedure adopted was that based on the Flume datasets, sorting fourteen consecutive
135 hourly peak discharges in the rainy season. In this procedure, Ks is estimated by applying
136 of the Darcy's law equation. According to Pinto et al. (2015) and Libohova et al. (2018),
137 the hydraulic gradient may be estimated by the difference elevation between the gauging
138 station and the highest elevation of the catchment and this value is assumed being
139 constant. This procedure can be applied if only instantaneous peak discharge values were
140 selected during the rainy season, meaning that the soils were close to saturation. In this
141 case, the water flows throughout the catchment as the "soil column" (Libohova et al.
142 2018). The derived Ks values varied from 1.3 to 23.4 mm h^{-1} in the AFMC.

Overall, the saturated zone encompasses the fractured massive rock gneiss, with good permeability of saprolite (Menezes et al. 2014). These geological features characterize the AFMC's capability for groundwater storage and transmittance. In general, the AFMC can be considered as a representative catchment located at elevations higher than 1,400 m within Mantiqueira Range geomorphological domain, with soils, vegetation, topography, weather, and geology being most representative of the region.

Regarding the water table depth in a neighbor micro-catchment within the LCW, Oliveira (2014) monitored the water table level in 7 piezometers, and in the 2009-2011 period, it had varied from 0.8 to 1.6 m (Figure 2). Thus, there are indicators that the depth of the subsurface unconsolidated geology is around 1.0 – 1.5 m.

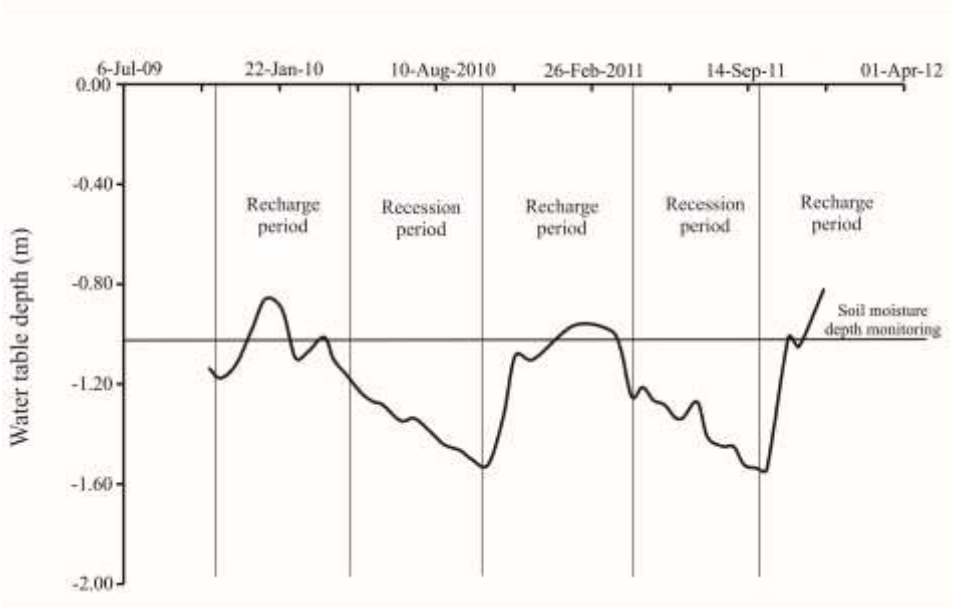

Figure 2. Average water table depth between 2009 and 2011 in an AFMC neighboring micro-catchment also located in the Lavrinha Creek Watershed as observed by Oliveira (2014) (see the piezometers' location in Fig. 1).

158 The AFMC displays an average slope of 35% and altitude varying between 1475
159 m and 1685 m. It has the following soil-landscape characteristics: shallow to moderately
160 deep soils (Haplic Cambisol – Inceptisols with solum varying from 0.70 to 1.20 m), with
161 high concentration of organic matter in the 0-0.5 m layer; the parent material being
162 granite-gneiss (Menezes et al. 2014); topography is commonly undulating, strongly
163 undulating or mountainous, and the basin shape is narrow, with a circularity index of
164 1.244.

165

166 **2.3 Meteorological condition**

167 From 2006 to 2012, the meteorological variables (precipitation, air temperature
168 and relative humidity, atmosphere pressure, air density, dew point, wind velocity and
169 direction, and global solar radiation) were recorded at the LCW by two standard
170 automatic meteorological stations separated by a distance of 740 m (Figure 1). The
171 Köppen climate type for Mantiqueira Range is Cwb, which can be summarized as
172 temperate highland tropical climate with dry winters and rainy summers. The mean
173 annual observed temperature between 2006 and 2012 was 16^{o}C and was calculated based
174 on the hourly values recorded by the meteorological station 2 (Figure 1). The minimum
175 and maximum annual mean observed temperatures were 10°C and 23°C and were
176 calculated by taking the minimum and maximum daily values from the same
177 meteorological station. From 2006 to 2012, annual precipitation ranged from 1841 mm
178 to 2756 mm; on average, it corresponded to 2311 mm, with 89.5% of this amount
179 concentrated between September and March. Thus, there is a marked dry period, which

180 begins in April and ends in August and the hydrological year for the studied region is
181 defined as the period from September in one year to August in the following year.

182 **3 Methods**

183 **3.1 Components of water balance at the AFMC**

184 The AFMC was monitored from June 2009 to December 2011, within the scope
185 of a wider research and development project sponsored by the Minas Gerais state
186 Electrical Energy Company (CEMIG) and the Electrical Energy National Agency
187 (ANEEL). This monitoring effort allowed to account the elements of water balance using
188 two complete hydrological years. The datasets encompassed canopy rainfall interception,
189 soil moisture, weather, streamflow, and other soil and vegetative measurements carried
190 out during the same period.

191 **Meteorological elements and evapotranspiration**

192 The monitoring involved meteorological variables, which were recorded by a
193 Campbell automatic weather station (model: "WeatherHawk" station; Station 1 – Figure
194 1) installed in a clear-cut area 30 m from the AFMC. It was assumed that these data sets
195 are representative of the conditions at 2 m above the forest canopy (Fleischbein et al.
196 2010; Muñoz-Villers et al. 2012; Salemi et al. 2013).

197 Using the observed meteorological variables and the procedures used by Allen et
198 al. (1998), the Penman-Monteith model (Monteith, 1964) was applied to estimate daily
199 evapotranspiration (ET, mm d^{-1}) for the studied site:

$$ET = \frac{\Delta \cdot Rn + \rho \cdot cp \cdot (es - e) \cdot g_a}{\lambda \cdot \left(\Delta + \gamma \cdot \left(1 + \left(g_a / g_c \right) \right) \right)} \quad (1)$$

where Δ is the slope of the saturation vapor pressure curve (kPa $°C^{-1}$); λ is the latent heat of water vaporization (MJ kg^{-1}); Rn is the net radiation (MJ m^{-2} d^{-1}); ρ is the moist air density (kg m^{-3}); cp is the specific heat at a constant pressure (1.013 kJ kg^{-1} $^oC^{-1}$); es is the saturation vapor pressure (kPa); e is the current vapor pressure (kPa); g_a is the aerodynamic conductance (m s^{-1}); g_c is the conductance of water vapor in the canopy (m s^{-1}); and γ is the psychrometric constant (kPa $°C^{-1}$).

It was necessary to calculate the Rn, based on latitude, altitude, leaf area index, and global solar radiation, according to the following equations (Yin et al. 2008; Allen et al. 1998):

$$Rn = Rsw + Rlw \quad (2)$$

$$Rsw = Rg \cdot (1 - \alpha) \quad (3)$$

$$Rlw = \left(\left(0.9 \cdot \frac{n}{N} \right) + 0.1 \right) \cdot \left(-0.34 + \left(0.14 \cdot \sqrt{e} \right) \cdot K_{S-B} \cdot \left(T_{air} + 273 \right)^4 \right) \quad (4)$$

Rsw and Rlw are short and long wave radiation (MJ m^{-2} d^{-1}) , respectively; Rg is the global solar radiation, which was monitored at our weather station every 60 minutes (MJ m^{-2} d^{-1}); α is the albedo, considered constant and equal to 0.12 for forests as assumed by Muñoz-Villers et al. (2012); K_{S-B} is the Stephan-Boltzman constant (4.903 x 10^{-9} MJ K^{-4} m^{-2} d^{-1}); n is the actual duration of sunshine (hours); N is the maximum duration of sunshine (hours); and T_{air} is the air temperature (^oC).

For g_a calculation, an average canopy height of 8.6 m was considered based on observed forest data in the catchment (Allen et al. 1998). The conductance of water vapor in the canopy (g_c) was obtained by:

$$g_c = g_S \cdot LAI \quad (5)$$

where g_s is the stomatal conductance, and LAI is the leaf area index ($m^2\ m^{-2}$). The values of g_s were estimated by Pereira et al. (2010) who studied another forested site within the LCW at similar altitudes during the dry periods of 2008 and 2009.

The LAI was monitored with a LAI2000 Plant Canopy Analyzer (Licor Biosciences, Nebraska, USA) and a sensor with a viewing angle of 180 degrees. To reduce the uncertainties of the LAI measurements, a reading with a clear sky was firstly performed as a reference. Then, 10 more readings were taken, spaced approximately 10 m apart within the forest in a 20 m x 90 m area, following a straight path through the center of the area to avoid boundary effects, searching to cover the entire area. This procedure was repeated twice in a roundtrip path for 20 readings, always performed before 09:00 a.m. or after 3:00 p.m., and avoiding cloudy days, performed approximately twice a month.

A comparative analysis was carried out between the evapotranspiration modeled based on the equations from 1 to 5 (ET) and the evapotranspiration obtained based on the water balance method conducted during the months of the dry period (from April to August of 2010 and 2011) (ET_{WB}). This procedure implies that ET from the water balance was calculated mainly based on the changes in soil-water storage in the 0 - 1.0 m layer (control layer) and in observed rainfall events that normally do not have a significant

241 impact on streamflow, mostly returning to the atmosphere by evaporation from canopy
242 (Tomasella et al. 2008). Thus, ET can be estimated by the following water balance
243 equation:

244 $$ET_{WB} = TF - \Delta S_{USZ} + C \quad (6)$$

245 where ET_{WB} represents the evapotranspiration from this water balance (mm), TF is the
246 throughfall (mm), ΔS_{USZ} is the soil-water storage change in the 0-1.0 m layer (in mm)
247 that was taken approximately every 20 days, and C is the rainfall canopy interception.

248 Aiming to strength the validation of the ET estimated in this study, the daily
249 estimated values were accounted for 8-day (ET 8-day), and then were compared to the
250 values extracted from MODIS/Terra Net Evapotranspiration 8-day with 500-m of spatial
251 resolution, considering the two studied hydrological years (ORNL DAAC, 2018; Running
252 and Mu, 2017). The datasets from MODIS are also estimated based on Penman-Monteith
253 by means of an algorithm developed by Mu et al. (2007). These datasets are validated
254 based on ground meteorological observations and Eddy Covariance flux towers around
255 the world (Mu et al. 2007).

256

257 **Rainfall canopy interception**

258 Twenty-five rain-gauges for throughfall measurement (model: “Ville de Paris”,
259 manufactured with a 415 cm^2 orifice), were installed 1.5 m above the ground across the
260 catchment (Figure 1). Throughfall measurements were taken at approximately noon time

261 of each rainy day in an attempt to reduce problems with accumulation and overlap of
262 rainfall events.

263 Rainfall events with less than 20 mm and separated by at least 24 hours were taken
264 to estimate the maximum canopy storage capacity (Sc) (Cuartas et al. 2007) by means of
265 a linear regression between the average throughfall (y) and gross precipitation (x). The
266 Sc corresponds to the x value when y = 0. For the AFMC, Sc was equal to 1.58 mm d^{-1}.

267 From these readings, the canopy rainfall interception (C) (mm) was determined
268 by the following equation (Guimire et al. 2017):

269 $$C = P - TF - Stf \quad (7)$$

270 where P is the gross precipitation (mm), TF is the throughfall (averaged from 25 gauges)
271 (mm), and Stf is the stemflow which was not measured in this study since it is not
272 significant from a water balance point of view (Zimmermman et al. 2013).

273 On computing evapotranspiration (ET) through the water balance, the interception
274 loss (C) were added to the evapotranspiration estimated by Penman-Monteith when the
275 canopy was not saturated (C < Sc); otherwise, when the canopy was saturated only C
276 values were computed for ET, since under this condition, the transpiration can be
277 negligible (Tomasella et al. 2008; Shuttleworth, 1992).

278

279 **Soil water storage (SWS)**

280 Twenty-five soil moisture probes (type PR2/6¨ Delta-T Devices, London, UK,
281 accuracy 0.04 m^3 m^{-3}), calibrated according to Evett et al. (2006), were installed in the

same location of the rain-gauges for measuring the volumetric soil moisture in depths of 0.10 m, 0.20 m, 0.30 m, 0.40 m, 0.6 m and 1.0 m. As this device does not make automatic reading of the soil moisture, we adopted a time interval between the readings of approximately 20 days. Soil water storage (SWS, in mm) for each date (t) and its change between consecutive readings were calculated, respectively, by:

$$SWS_t = \sum_{i=1}^{n}\left(\frac{\theta_i + \theta_{i+1}}{2} \times h\right) \quad (8)$$

$$\Delta S_{soil} = SWS_{(j+t)} - SWS_{(t)} \quad (9)$$

where θ_i and θ_{i+1} are, respectively, the soil moisture in the depth i and in the follow depth ($m^3\ m^{-3}$), n is the number of layers (0 - 0.10 m; 0.1 - 0.2 m; 0.20 – 0.30 m; 0.30 – 0.40 m; 0.40 – 0.60 m; 0.60 – 1.0 m), h is the layer thickness (mm) and j is the time interval. In addition, we calculated the SWS for the layers of 0 - 0.20 m (surface layer), 0.20 – 0.60 m (intermediate layer) and 0.60 – 1.0 m (deeper layer) for studying the statistical relationship with the streamflow components.

Streamflow

The streamflow in the AFMC was monitored by means of a Parshall flume and an automatic water level sensor (model WL16 Global Water Instrumentation, California, USA). The discharges were recorded at 60-min by the datalogger of the instrument. The hydrographs analyses were based on the daily discharge value. The procedure was carried out by the separation of the baseflow from the total streamflow by identification of the inflexion point in the recession limb from the baseflow and the beginning of the overland

303 flow (Hingray et al. 2014). The baseflow follows the fundamentals of the Maillet
304 exponential equation (Dewandel et al. 2002):

305 $$\frac{dQ}{dt} = -\alpha \cdot Q \quad (10)$$

306 $$Q_t = Q_o \cdot \exp(-\alpha \cdot \Delta t) \quad (11)$$

307 Q_0 is the initial flow rate ($m^3\ s^{-1}$), Q_t is the flow rate ($m^3\ s^{-1}$) at time t (daily), α (d^{-1}) is the
308 recession coefficient, and Δt the number of days between consecutive flows.

309 The baseflow contribution to the streamflow was assessed using the baseflow
310 index (BFI) (Clark et al. 2014; Muñoz-Villers and McDonnell, 2013; Caballero et al.
311 2012) as follows:

312 $$\mathrm{BFI}(\%) = \left(\frac{\text{total volume of baseflow}}{\text{total volume of streamflow}} \right) \times 100 \quad (12)$$

313 In order to assess possible connections between streamflow, overland flow, and
314 baseflow with evapotranspiration, throughfall, and SWS at three different soil layers (0 –
315 0.20 m; 0.20 – 0.60 m; 0.60 to 1.0 m), multiple regressions using the stepwise approach
316 based on the Akaike Information Criterion (AIC) for the selection of independent
317 variables were fitted. These analyzes have focused to demonstrate how the unsaturated
318 zone can influence the streamflow in a TMCF like the AFMC.

319

320 **3.2 Water balance**

321 The daily water balance was calculated based on the following equation:

322 $$S_{AFMC\ (i+1)} = S_{AFMC\ (i)} + P_{(i)} - ET_{(i)} - SF_{(i)} \quad (13)$$

where S_{AFMC} (i) is the water storage in AFMC in i^{th} day (mm), $S_{AFMC\ (i+1)}$ is the water storage in AFMC in the following day (mm), $P_{(i)}$, $ET_{(i)}$ and $SF_{(i)}$ are, respectively, the rainfall, evapotranspiration, and streamflow in the i_{th} day; all variables in mm.

The potential groundwater recharge in AFMC (GS) was estimated based on the time interval adopted for soil moisture measurements (≈ 20 days). The following equation was applied:

$$GS_{(j)} = \Delta S_{AFMC\ (j)} - \Delta S_{soil\ (j)} \quad (14)$$

$\Delta S_{AFMC\ (j)}$, $\Delta S_{soil(j)}$ and $GS_{(j)}$ are, respectively, the water storage variation in AFMC accounted based on equation 13, in the soil-layer of 0 – 1.00 m (unsaturated zone), accounted based on equation 9, and potential groundwater recharge, in the j^{th} period of approximately 20 days.

The 0 – 1.0 m layer was considered for ΔS_{soil} measurement as the maximum observed solum depth being 1.20 m (Menezes et al. 2014) and the saturated zone of the catchment varied from 0.8 m and 1.6 m during the studied hydrological years (Figure 2). These assumptions allowed the estimation of potential groundwater recharge that occurred during the time interval of the soil moisture readings.

4 Results

4.1 Water balance elements at the AFMC between 2009 and 2011

Rainfall and throughfall

Figure 3a shows the temporal behavior of the gross precipitation (meteorological station 1 – Figure 1) and the average throughfall and its respective standard errors (mm), calculated based on the spatial variability of the records, between 2009 and 2011. Figure 3b presents the mean monthly precipitation and respective standard deviation for the LCW (meteorological station 2) based on the monitored period from 2006 to 2012. The observed gross precipitation for the hydrological year of 2009-2010 was 2,250 mm and for the 2010-2011 hydrological year, 2,756 mm.

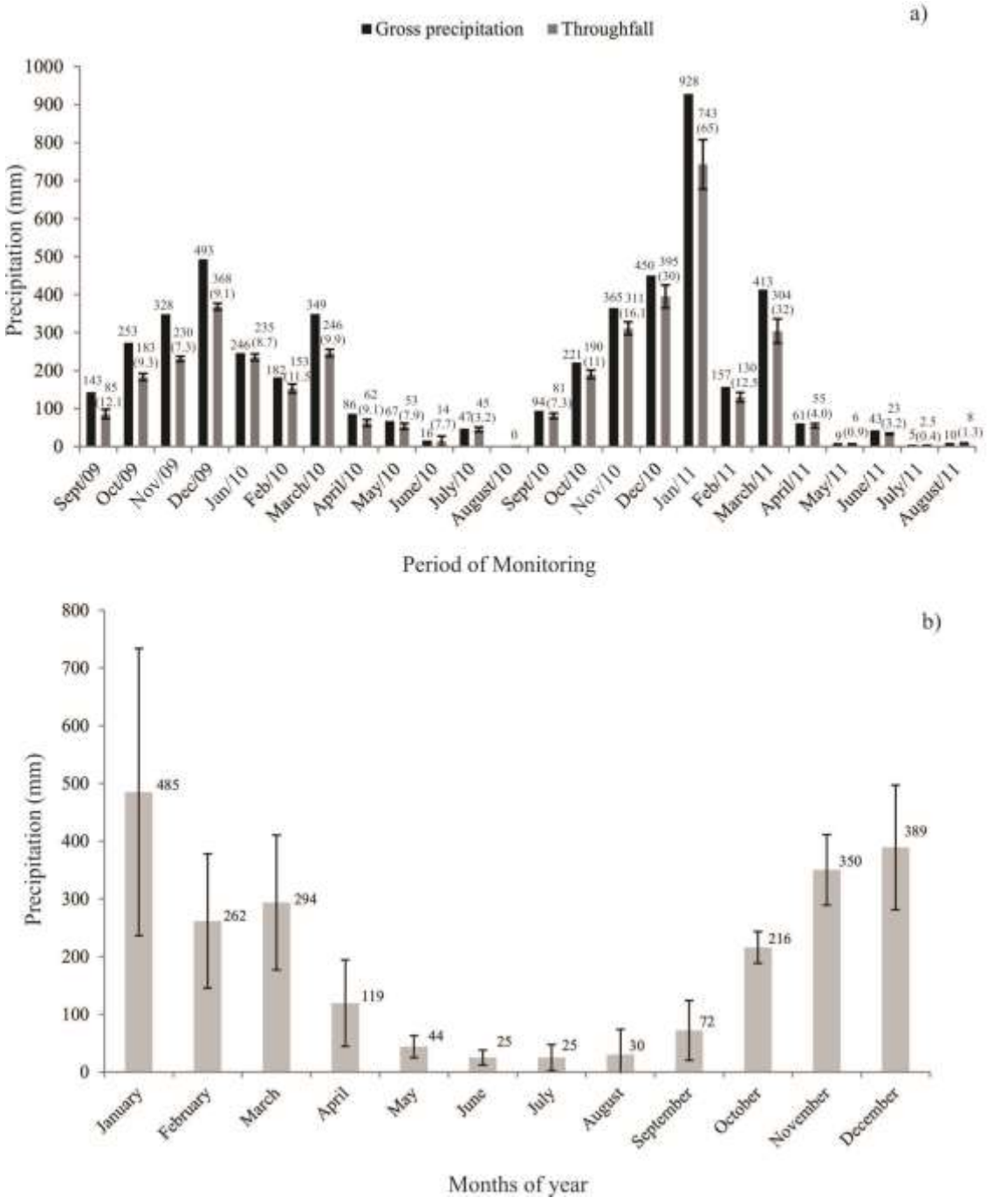

Figure 3. Monthly gross precipitation, throughfall and its standard errors as observed in the AFMC during the hydrological years of 2009-2010 and 2010-2011 (a) and average monthly gross precipitation and respective standard deviation as observed in the Lavrinha Creek Watershed from 2006 to 2012 (b).

In Table 1, it is presented the results of the studied meteorological variables split into seasons of the year. It was observed for the hydrological years of 2009/2010 and 2010/2011, C/P ratio of 21.3 and 20.5%, respectively. For the wet season of 2009-2010, it was observed 20.9% of interception, whereas for 2010/2011, this value was practically the same, 20.8%.

Table 1.

Evapotranspiration

Daily average values of ET modeled (ET) (equation 1) and ET from the water balance carried out during the dry periods (April – September/2010 and 2011) (ET_{WB}) (equation 6) were analyzed to produce the statistical relationship presented in Figure 4a. In addition, the ET 8-day values estimated in this study were compared to the ET 8-day extracted from MODIS Global Terrestrial Evapotranspiration Product (ORNL DAAC, 2018; Running and Mu, 2017) and the results are presented in Figure 4 (b, c). Both validation procedures are essential for the study since ET accounts for the greatest portion of the water balance.

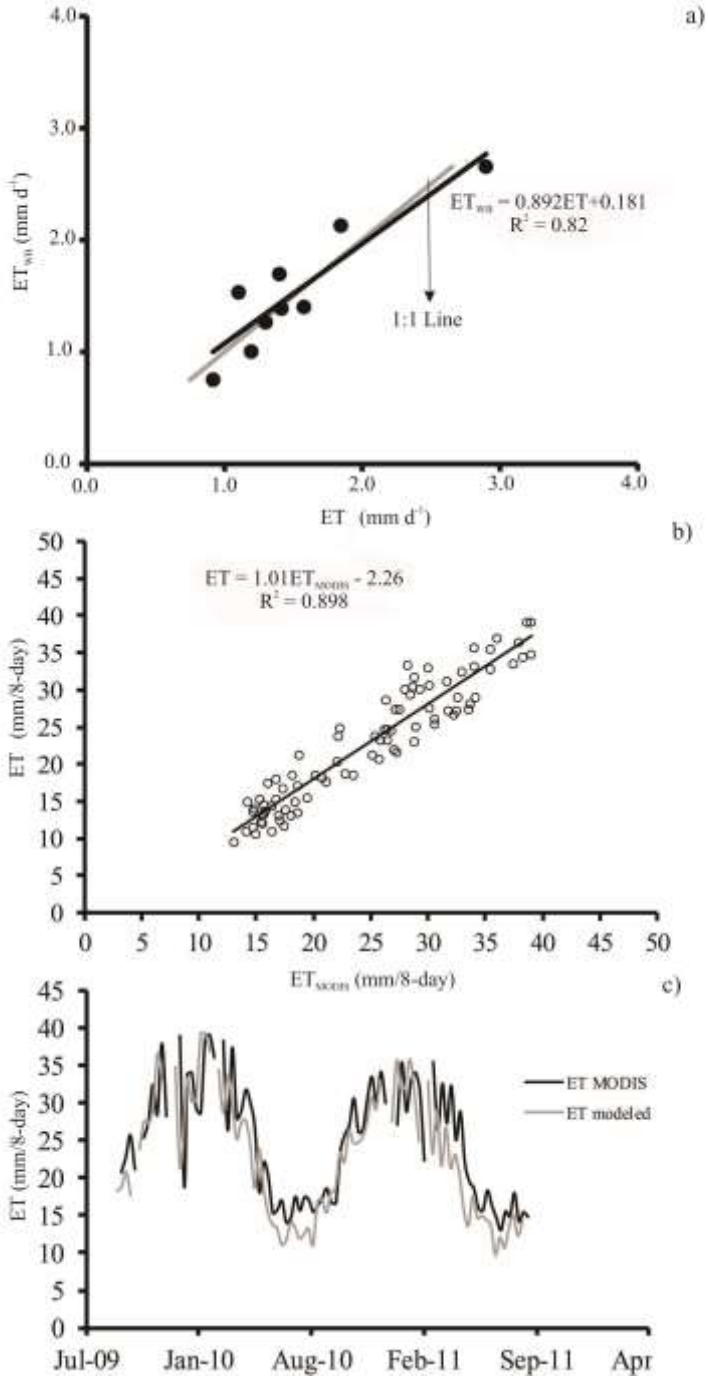

373

374 **Figure 4.** Relationship between evapotranspiration modeled (ET) and evapotranspiration
375 from water balance (ET_{WB}) during the dry periods in AFMC site (a), and comparison
376 between ET 8-day modeled and ET 8-day from MODIS (b, c).

377 The ET averaged up to 50% of P in the AFMC and varied between the two
378 hydrological years: from 1172 mm $year^{-1}$ (54.8% of P) to 1208 mm $year^{-1}$ (45.3% of P),
379 respectively, for 2009/2010 and 2010/2011.

380 Leaf Area Index (LAI) throughout the monitoring period (monthly values) is
381 presented in Figure 5a, which varied from 2.8 to 5.2 $m^2 m^{-2}$. Figure 5 also shows ET (b),
382 air temperature (c), and net radiation (d) throughout the study period for the AFMC,
383 showing the correlated patterns of the meteorological variables and the ET.

384

385 **Figure 5.** Temporal behavior of the leaf area index (monthly) (a), evapotranspiration
386 (daily and monthly values) (b), air temperature (hourly, daily and monthly values) (c),
387 and net radiation (daily and monthly values) in the AFMC throughout the studied period
388 (2009 to 2011).

389

390 **Soil water storage (SWS) and streamflow**

391 Figure 6 presents the temporal dynamics of SWS and its respective limits
392 calculated based on the standard deviation of the readings from the twenty five sampling
393 points in the AFMC for the layers of 0 – 0.20 m, 0.20 – 0.60 m and 0.60 – 1.0 m.

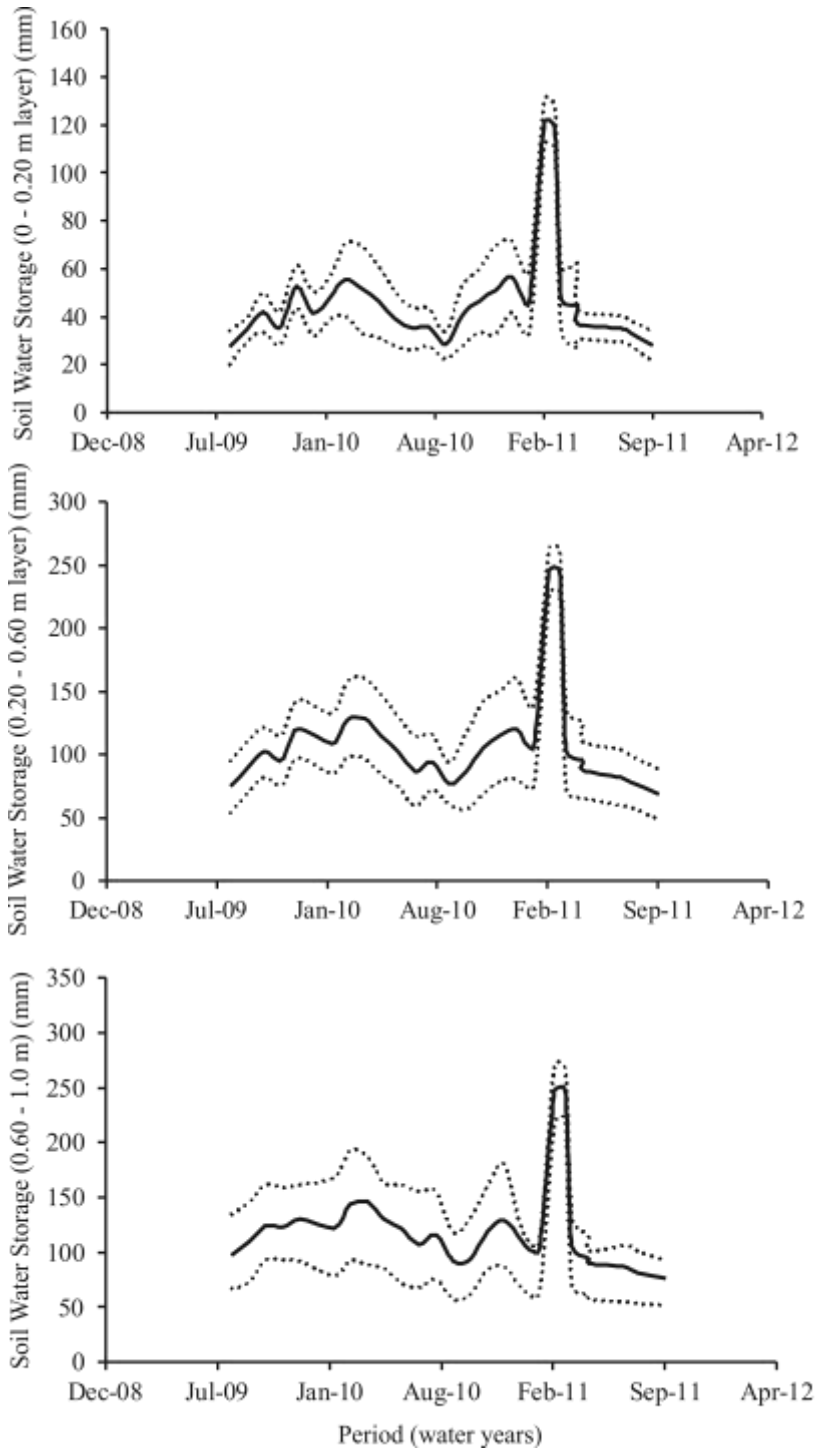

394

395 **Figure 6.** Soil Water Storage dynamics (average and upper and lower limits calculated
396 based on the 25 locations for soil moisture measurement – Figure 1) throughout the
397 hydrological years from 2009 to 2011.

The distribution of rainfall intensity and streamflow and baseflow are presented in Figure 7 in a daily time-step. Here it is possible to observe a predominance of rainfall intensity values lower than 5 mm h^{-1}, in both hydrological years and only a few events higher than 20 mm h^{-1}. The seasonality of the rainfall is clearly transferred to the streamflow, with the highest peak discharges observed in the summer.

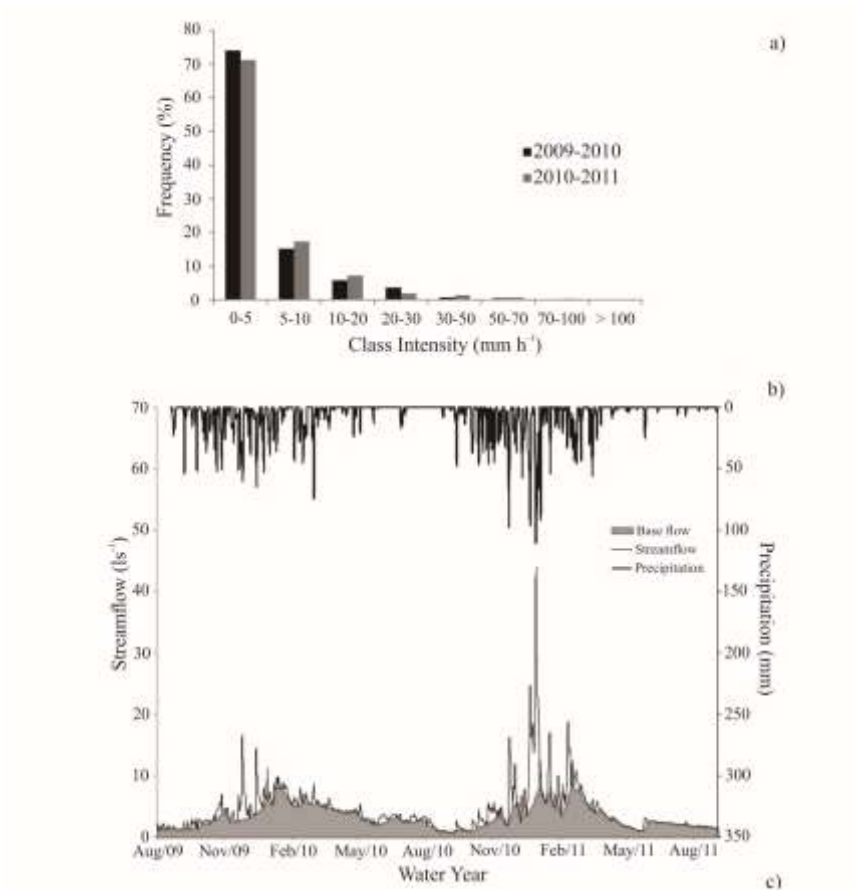

Figure 7. Classes of rainfall intensity frequency (a) and daily streamflow, base flow and rainfall (b) throughout the hydrological years in the AFMC.

The baseflow index (BFI) values are presented in Table 2 for both wet and dry seasons calculated for the AFMC. In this study, the BFI was 0.77 and 0.70, respectively, for the hydrological years of 2009/2010 and 2010/2011.

Table 2.

Regarding the possible connections between baseflow and/or overland flow vs. soil water storage (SWS), evapotranspiration, and throughfall, stepwise multiple regressions were fitted and shown in Table 3.

Table 3

4.2 Water balance

Figure 8 shows the daily water balance at the AFMC calculated throughout the two hydrological years. Taking both Table 4 and Figure 8, it is possible to infer about potential groundwater recharge in the catchment throughout the hydrological years. Based on the water storage in the AFMC and the changes on soil-water storage up to 1.0 m in depth (ΔS_{soil}), we estimated the potential GS by application of the equation 14. During the wet seasons (Oct-March), with the occurrence of rainfall, the positive changes in water storage can also be observed as well as increase in the AFMC's water storage (Figure 8). In 2009/2010 hydrological water, a potential recharge of 403.8 mm was estimated, and for 2010/2011, 710.5 mm. In addition, a positive water storage stands out in the end of the hydrological years, with 203 mm (9.5% of P) and 554.5 mm (20.9% of P), respectively.

Figure 8. Daily water balance variation, potential groundwater recharge and daily rainfall in the AFMC during the hydrological years of 2009/2010 and 2010/2011.

Table 4.

5 Discussion

5.1 Water balance elements at the AFMC between 2009 and 2011

Rainfall and throughfall

A seasonality behavior of the gross precipitation and throughfall could be highlighted in the AFMC, following the rainfall pattern of the region, which is characterized by a wet (summer) and a dry (winter) seasons. Comparing gross precipitation observed in the AFMC to the average value observed in the LCW (2311 mm ± 470 mm) (Figure 3b), it can be inferred that the 2009-2010 hydrological year was closer

447 to the expected rainfall pattern for the Mantiqueira Range region. For hydrological year
448 of 2010/2011, it was observed a total rainfall considerably higher than the average along
449 with a greater concentration of rainfall in the wet season (92% of the total vs. 84%
450 observed for 2009/2010 hydrological year). These differences can be partially attributed
451 to an anomalous value observed in January 2011 (928 mm), which is larger than the upper
452 boundary of the 75% inter-quartile for this month (Figure 3b). Its occurrence was
453 attributed to a specific weather condition that predominated over southeastern Brazil, a
454 South Atlantic Convergence Zone episode associated with higher temperatures over the
455 Subtropical Atlantic Ocean, which contributed with greater moisture in the atmosphere,
456 and thus more rain for the coast of the region and surroundings (Marengo and Alves,
457 2012).

458 One of the main sources of error in gross precipitation monitoring is the wind
459 influence, which was considered negligible due to the low annual average value in both
460 stations (1.55 m s^{-1}). Another important source is the spatial variability due to
461 microclimates formed in mountainous landscape and the rainfall events provoked by
462 orographic effects. A comparison between these stations, which are separated by 740 m,
463 demonstrated a difference of 55 mm (2.4% of the total) and 105 mm (3.8%), respectively,
464 for the first and second hydrological years. Thus, these values demonstrate an acceptable
465 difference for gross precipitation over LCW.

466 Overall, rainfall canopy interception in relation to rainfall (C/P) varied slightly
467 between the hydrological years, with an average value of 20.9% (Table 1). In other studies
468 conducted in TMCF sites similar results were observed, such as Ghimire et al. (2017), in
469 Madagascar, and Muñoz-Villers et al. (2012), in Mexico. On the other hand, Salemi et al.

(2013) found a C/P ratio of 33% for a TMCF site in "Serra do Mar" region, with an altitude under 1,100 m. This difference is related to the species found in the site studied by Salemi et al. (2013), highlighting its larger leaves, a canopy more closed and species' morphology with greater biomass.

Standard errors related to throughfall are also depicted in Figure 3a for the AFMC. According to Munõz-Viller et al. (2012), the main source of uncertainty for these records is the spatial variability below the canopy. The results found here indicate that there was low variability of these data from most rain gauges, especially for the first hydrological year. This observed spatial variability for throughfall also demonstrates that the rain gauges are reasonably spatially distributed below the canopy.

Evapotranspiration

The ET model adopted in this study was capable of adequately estimate ET for the AFMC, supported by the meteorological data, and stomatal conductance estimated based on observed leaf area index (Figure 5a). In Figure 4a, it is presented the relationship between ET and ET_{WB}. The hypothesis test of the unit slope and the intercept equaling to zero showed that the fitted regression line is not significantly different from the 1:1 line (p = 0.15 and 0.41, respectively, for the angular and linear coefficients). This means that the modeled ET values were close to those calculated from the water balance conducted

491 considering only the dry periods of the hydrological years, which was dominated by the
492 changes in soil water storage.

493 Figure 4 (b, c) shows the relationship between ET modeled in the study and ET
494 extracted from MODIS satellite for 8-day values (ET 8-day), showing a satisfactory
495 precision of the estimates (Figure 4b) along with an adherence between the two
496 throughout the time (Figure 4c). In general, ET MODIS values were slightly greater than
497 ET modeled by approximately 8.5%.

498 Evapotranspiration varied slightly between the two hydrological years, which is
499 consistent with a Dense Ombrophilous Forest, mainly due to the sites above the elevation
500 of 1,400 m. Clark et al. (2014) estimated ET values in the TMCF in the Andes region
501 varying from 1000 to 1300 mm $year^{-1}$, close to those values obtained in this study.
502 However, upon analyzing the water balance, through an approach similar to the one of
503 this study, in two TMCF sites in Mexico, Muñoz-Villers et al. (2011) estimated ET values
504 of approximately 790 mm for both their catchments.

505 For a TMCF site located in Serra do Mar, Salemi et al. (2013) found a ET/P
506 relation of 56% during a hydrological year; however, the authors did not monitor the soil
507 moisture, considering the variation of water storage in the catchment equal to zero in the
508 end of the hydrological year. The ET/P ratio in the AFMC was lesser in the 2010-2011
509 year, similar to that value found by Zema et al. (2018), who modeled the water balance
510 in a watershed located between 1,100 and 1,200 m using the AnnAGNPS model, obtained
511 a ET/P ratio of 45%. In the case of the AFMC, this can be justified by the large number
512 of rainy days in the period between November and March, which was associated with a
513 saturation of the canopy and a reduction on impact of transpiration during this period. A

514 detailed analysis of the precipitation records revealed that there were 2,463 mm of rainfall
515 during the aforementioned period. Out of the 151 days of the period, 92 (60.9%) were
516 found to be rainy compared to only 67 (44.4%) for the same period in the 2009-2010 year.
517 Therefore, we can state that there was a greater surplus water in the catchment available
518 to sustain the streamflow in this hydrological year.

519 It is important to highlight that all the meteorological variables present a marked
520 seasonality which is the most significant climatic feature of the region with implications
521 for the water balance. When evaluating ET throughout the time, it is possible see that it
522 follows the LAI, net radiation, and temperature oscillations (Figure 5), demonstrating the
523 importance of these meteorological variables to explain the water demand by the forest.
524 In wet season, LAI values have oscillated around 5 m^2 m^{-2}, and the daily
525 evapotranspiration (transpiration + wet-canopy evaporation) close to 4 mm d^{-1}. In the
526 winter, LAI values oscillated around 3 m^2 m^{-2} while ET, 1 mm d^{-1}. These oscillations are
527 expected for tropical and subtropical deciduous forests and occurs due to reduction in the
528 tree physiological activities in drier and cooler periods.

529 Both ET and P tended to increase over the summer, indicating atmospheric
530 conditions more favorable to both transpiration and evaporation of the rainfall intercepted
531 by the canopy. It is important to stress that, according to Shuttleworth (1992), the
532 participation of transpiration is greater under the conditions of a dry or moist canopy;
533 otherwise, with a saturated canopy, evaporation is predominant. In environments like the
534 AFMC, there is a predominance of colder and rainy weather due to its elevation (greater
535 than 1400 m) and proximity to the Atlantic Ocean coast. Thus, in summer (wet period),

536 the canopy moisture is close to saturation and it helps to sustain the greatest part of the
537 atmospheric demand.

538

539 **Soil water storage (SWS) and streamflow**

540 Soil water storage (SWS) seasonality in the AFMC is noticeable throughout the
541 monitoring period. In general, increasing SWS from the surface to the deeper layers and
542 greater dynamics in the 0-0.20 m layer can be observed. Also, the deeper the layer the
543 higher the SWS variability, which is also related to the greater influence of the forest root
544 system in depth (mainly in the dry season). Between February/March 2011, a strong
545 increase in SWS affected the AFMC, impacting the overland flow in the second
546 hydrological year, which was not observed with the same magnitude in the wet season of
547 2009-2010.

548 Pinto et al. (2015) studied the role of the Inceptsols, the dominant soil type in the
549 study area, on the LCW's hydrology based on micromorphology images and concluded
550 that both macro-porosity and interconnections between larger pores especially at the 0-
551 0.20 m layer are fundamental for infiltration capacity of these soils. It was observed that
552 there is a clear influence of the forest on soil porosity in this surface soil layer, while in
553 deeper soil layers there is greater micro-porosity (Pinto et al. 2015), which leads to a
554 greater redistribution of moisture, and thus higher variability in subsoil moisture (Figure
555 6 a, b, c).

556 Further analyzing the daily rainfall distribution and the respective streamflow in
557 the AFMC (Figure 7), the majority of the rainfall events has low intensity (more than 90%

558 rainfall events were lower than 10 mm h^{-1}). The greater intensity events were observed
559 for 2010-2011 hydrological year. In addition, a few rainfall events with intensity greater
560 than 50 mm h^{-1} were observed. The behavior of these rainfall events is similar to those
561 found by Salemi et al. (2013) and have low capacity to generate overland flow, especially
562 in a catchment entirely covered by a dense forest canopy. Examination of the SWS
563 (Figure 6) reveals extremely high values between January and March 2011, as a result of
564 more than 900 mm of rain.

565 The BFI behavior in the AFMC was similar to those observed at other TMCF sites,
566 with baseflow having a significant participation in the streamflow, which is particularly
567 evident during the dry season. In these seasons, this coefficient was 0.84 and 0.89,
568 respectively, for 2010 and 2011. Clark et al. (2014), in analyzing a hydrological year for
569 a TMCF in the Andes with bedrock/fractured bedrock as geological backgrounds,
570 observed BFI oscillating from 0.60 in the wet season to 0.83 in the dry season. They
571 concluded that the baseflow has been the main factor responsible for streamflow
572 maintenance. Caballero et al. (2012), in studying a TMCF in Costa Rica, also found
573 results similar to those of this study, with a BFI around 0.80. They concluded that the
574 participation of the baseflow was significant because of the amount of groundwater stored
575 throughout the rainy season. Thus, we have demonstrated that the BFI values in the
576 AFMC are quite consistent with other studies carried out in TMCF sites around the world,
577 including Hugenschmit et al. (2014), Clark et al. (2014), Caballero et al. (2012), and
578 Crespo et al. (2011) for northern Thailand, eastern Andes (southern Peru), Costa Rica
579 (Central-America), and Equatorial Andes, respectively.

Some insights from Table 3 can be highlighted. Firstly, the correlations were significant according to the *t*-test. Stepwise regression demonstrated that the overland flow could be well explained by the throughfall and SWS at 0.20 – 0.60 m layer. However, for the baseflow only SWS at 0.60 – 1.0 m layer was significant and positively correlated. The positive correlation between overland flow and SWS at 0.20 – 0.60 m can be explained based on the fact that throughfall infiltrates rapidly through 0 – 0.20 m layer via macro-pores (Pinto et al. 2015), whose breakthrough leads to a saturation in the sub-surface layer (0.20 – 0.60 m) that leads to overland flow. The SWS at the deepest layer (0.60 – 1.0 m) presented a significant but negative correlation with overland flow; whereas for baseflow, it was significant but positive, suggesting that this layer is well connected to the baseflow. In this sense, we can infer that SWS at the 0.60 – 1.0 m layer played an important role in the saturated zone water storage capability in the AFMC.

5.2 Water Balance

A marked predominance of positive water storage in the catchment in the wet seasons (2009/2010 and 2010/2011) stands out. Larger values for wet season of 2010/2011 can be observed as a result of the significant amount of rainfall observed in the region in this period. Additionally, we can also see that the AFMC is very sensitivity to the rainfall occurrence, being the water balance elements on wet season more dynamic, showing a quick respond even for slight rainfall occurrence.

601 The results presented in Table 4 allow us to demonstrate that water storage in the
602 AFMC has an important role for the baseflow. The capability of the AFMC for water
603 storage during the wet season, and how the catchment deals with it throughout the
604 hydrological years are fundamental for maintenance of the streamflow in the recession
605 period. Muñoz-Villers et al. (2016) studied the baseflow behavior on the basis of water
606 transit time, by means isotope hydrology in a TMCF in Mexico. They found that the
607 resident time in the saturated zone of the catchment varied from 1.2 to 2.7 years,
608 concluding on the possible controls of baseflow by long subsurface flow paths that are
609 related to the permeability of soil-bedrock interface. Clark et al. (2014) and Caballero et
610 al. (2012), both carrying out studies in TMCF sites in Andes and Central America,
611 respectively, observed a significant participation of the baseflow, which indicates that it
612 sustains the streamflow throughout the dry period. Clark et al. (2014) further discussed
613 aspects regarding the hydrogeology of the catchment, showing a considerable amount of
614 groundwater along with possible existence of fractures in the bedrock.

615 Muñoz-Villers et al. (2016) characterized a TMCF site in Mexico with a soil-
616 bedrock interface along with saturated hydraulic conductivity (Ks) varying from 1 to 15
617 mm h^{-1} for 65% of the catchment's area. Based on these Ks values, they characterized the
618 transition between the saprolite and bedrock as of high permeability, favoring the
619 groundwater storage and movement in the catchment. A similar relation may be
620 established for the studied AFMC as Ks values ranged from 1.4 to 23.7 mm h^{-1}, and
621 fractured bedrock, colluvial deposits, and permeable saprolite are the main geological
622 features for Mantiqueira Range region (Pinto et al. 2015). Thus, there are indications that
623 the baseflow in the AFMC is sustained by hydrogeological functions described as of good

624 permeability in the transition between saprolite and bedrock, not linked to short-term
625 fluctuations.

626 In addition, the AFMC has a narrow shape (the circularity index is 1.244), and
627 under this condition, the hydrological connectivity between hillslopes and the drainage
628 systems is higher than for rounded catchment shapes, which increase the frequency of
629 water table formation (Hrachowitz et al. 2009).

630 Differences in the water balance elements between the two hydrological years
631 could be noticed. The greater amount of GS estimates is linked to: (i) the total
632 precipitation in 2010/2011 is much greater than what was observed for 2009/2010,
633 besides more concentrated. In January/2011, it was observed more than 900 mm and a
634 greater number of rainy days, affecting the water balance components in a different
635 manner as compared to 2009/2010; (ii) these impacts could be observed on the greater
636 streamflow, lower canopy interception and ET, saturation of the soil profile and thus, a
637 larger amount of water surplus available for storage in the AFMC. Therefore, we could
638 observe a more significant GS for the AFMC, which was reflected in a greater baseflow
639 participation in the dry season of 2011, given by the greatest BFI observed during the
640 studied period (0.89 – Table 2).

641 Some limitations need to be highlighted in this study. First of all, we did not
642 evaluate the impact of condensation on the water balance, as done by Clark et al. (2014),
643 who demonstrated that almost 10% of the baseflow is formed by this source of water.
644 Furthermore, similar to Clark et al. (2014), Muñoz-Villers et al. (2012), Caballero et al.
645 (2012) and Salami et al. (2013), deep percolation into the groundwater system was not
646 detailed in a daily time-step and we calculated a potential recharge based on the readings

of soil moisture for each 20 days (equation 15). However, the existence of a great water storage capacity in the AFMC was demonstrated based on the daily water balance, which was the first study with this time resolution encompassing two complete hydrological years in this kind catchment in Brazil.

Despite the above limitations, our TMCF site is within a Biosphere Reserve recognized as one of the most important ones on the planet, mainly due to its hydrologic behavior. The datasets involved in this study bring important insights into the water balance and streamflow connections. Our findings show some important novelties: (i) the baseflow is the primary source for streamflow and it was not linked to short-term fluctuations of rainfall; (ii) we could demonstrate that the catchment can store water in the wet season aiming to maintain the permanent streamflow even in the recession phase of the hydrological year; (iii) these results can be applied to support ecological services in mountainous catchments in southeastern Brazil, giving the necessary scientific support for protection of the Atlantic Forest biome, showing its relevance in reducing harm effects from droughts that have threatened this Brazilian region in recent years.

6 Conclusions

This study is among the first efforts to understand the water budget in a mountainous forest located above 1400 m asl in Brazil. Baseflow is found to be the main hydrological element in this catchment that maintains the streamflow, not only during the recession phase, but also for longer periods especially during prolonged droughts. The baseflow is attributed to groundwater storage capacity that has helped sustain the streamflow. Major findings of this study are summarized as follows:

669 a) Rainfall interception by canopy (C) was significant and corresponded to 21.3%
670 and 20.5% of the gross precipitation (P) in wet seasons of 2009/2010 and
671 2010/2011 hydrological years, respectively, with an average of 20.9% throughout
672 the hydrological years; while evapotranspiration corresponded to an average of
673 50% of P, with a greater demand in the wet season of 2010/2011 due to both
674 greater interception and the atmospheric demand;

675 b) Streamflow accounted for 34.8% of P, with high predominance of baseflow, being
676 77% and 70%, respectively, for 2009/2010 and 2010/2011 hydrological years;
677 noteworthy was a slightly greater predominance of overland flow in the second
678 hydrological year as compared to the first hydrological year due to greater amount
679 and more intense rainfall events;

680 c) Both hydrological years closed with a positive water storage in the Atlantic Forest
681 Micro-Catchment, corresponding to 9.5% and 20.9% of P for 2009/2010 and
682 2010/2011, respectively, with an average of 15.2%;

683 d) The predominance of water storage in the Atlantic Forest Micro-Catchment over
684 the two hydrological years was demonstrated by means of a daily water balance,
685 showing the resilience of this environment in terms of water yield and baseflow
686 maintenance during dry seasons. Based on this result, the baseflow is predominant
687 and indeed is controlled by a complex hydrogeological system, highlighting the
688 permeability of the soil-bedrock interface that allows a significant groundwater
689 storage in this ecosystem.

690 **Acknowledgments**

691 The authors thank CEMIG/ANEEL (R&D 176 Project), FAPEMIG (PPM X – 415/16)
692 and CNPq (301556/2017-2) for sponsoring this project. We also appreciate the comments
693 provided by Catena Editorial Team and anonymous reviewers that have helped improve
694 the quality of this paper.

695

696

697

698

699

700

701

702

703 **References**

704 Allen, R.G., Pereira, L.S., Raes, D and Smith, M. 1998. Crop evapotranspiration –
705 guidelines for computing crop water requirements. Roma: FAO Irrigation and Drainage,
706 56.

707

708 Bruijnzeel, L.A., Mulligan, M., Scatena, F.N. 2011. Hydrometeorology of tropical
709 montane cloud forests: emerging patterns. Hydrological Processes, 25, 465-498.

710

711 Bruijnzeel, L.A., Kappelle, M., Mulligan, M., Scatena, F.N. 2010. Tropical montane
712 cloud forests: state of knowledge and sustainability perspectives in a changing world.
713 691-740p. In: Bruijnzeel, L.A., Scatena F.N., Hamilton, L.S. (eds.). Tropical Montane
714 Cloud Forests. Science for Conservation and Management. Cambridge, Cambridge
715 University Press.
716
717 Caballero, L.A., Rimmer, A., Easton, Z.M., Steenhuis, T.S., 2012. Rainfall runoff
718 relationships for a cloud forest watershed in Central America: implications for water
719 resource engineering. Journal of the American Water Resources Association, 48 (5),
720 1022-1031.
721
722 Clark, K.E., Torres, M.A., West, A.J., Hilton, R.G., New, M., Horwath, A.B., Fisher, J.B.,
723 Rapp, J.M., Robles Caceres, A., Malhi, Y. 2014. The hydrological regime of a forested
724 tropical Andean catchment. Hydrology and Earth System Science, 18, 5377-5397. (DOI:
725 10.5194/hess-18-5377-2014).
726 Coelho, C.A.S., Cardoso, D.H.F., Firpo, M.A.F. 2015. Precipitation diagnostics of an
727 exceptionally dry event in São Paulo, Brazil. Theoretical and Applied Climatology. DOI
728 10.1007/s00704-015-1540-9.
729
730 Crespo, P., Bücker, A., Feyen, J., Vaché, K.B., Frede, H.G., Breuer, L., 2011. Preliminary
731 evaluation of the runoff processes in a remote montane cloud forest basin using mixing
732 model analysis and mean transit time. Hydrological Processes, 26, 3896-3910.
733

734 Cuartas, L.A., Tomasella J., Nobre, A.D., Hodnett, M.G., Waterloo, M.J., Múnera, J.C.,
735 2007. Interception water-partitioning dynamics for a pristine rainforest in Central
736 Amazonia: Marked differences between normal and dry years. Agricultural, Forest and
737 Meteorology, 145, 69-83.

738

739 Dewandel, B., Lachassagne, P., Bakalowicz, M., Weng, P.H., Al-Malki, A., 2002.
740 Evaluation of aquifer thickness by analyzing recession hydrographs. Application to the
741 Oman ophiolite had-rock aquifer. Journal of Hydrology, 274, 248-269.

742

743 Evett, S. R., Tolk, J. A., Howell, T. A., 2006. Soil profile water content determination:
744 axil response, calibration, temperature dependence, and precision. Vadose Zone Journal,
745 5, 894 – 907.

746

747 Fleischbein, K., Wilcke, W., Goller, R., Valarezo, C., Zech, W., Knoblich, K. 2010.
748 Measured and modeled rainfall interception in a lower montane forest, Ecuador. In: L.A.
749 Bruijnzeel, M. Kappelle, M. Mulligan, and F.N. Scatena, eds., Tropical Montane Cloud
750 Forests. Science for Conservation and Management. Cambridge, UK: Cambridge
751 University Press, 309-316.

752

753 Fleischbein, K., Wilcke, W., Valarezo, C., Zech, W., Knoblich, K. 2006. Water budgets
754 of three small catchments under montane forest in Ecuador: experimental and modeling
755 approach. Hydrological Processes, 20, 2491-2507. DOI: 10.1002/hyp.6212.

756

757 Fleischbein, K., Wilcke, W., Goller, R., Boy, J., Valarezo, C., Zech, W., Knoblich, K.
758 2005. Rainfall interception in a lower montane forest in Ecuador: effects of canopy
759 properties. Hydrological Processes, 19, 1355-1371. DOI: 10.1002/hyp.5562

760

761 Galindo-Leal, C., Câmara, I.G. 2003. Atlantic forest hotspot status: an overview. In: C.
762 Galindo-Leal, I.G. Câmara, eds. The Atlantic Forest of South America. Washington, DC:
763 Center for Applied Biodiversity Science, 3-11.

764

765 Ghimire, C.P., Bruijnzeel, L.A., Lubczynski, M.W., Ravelona, M., Zwartendijk, B.W.,
766 van Meerveld, H.J. 2017. Measurement and modeling of rainfall interception by two
767 differently aged secondary forests in upland eastern Madagascar. Journal of Hydrology
768 545: 212-225. doi: 10.1016/j.jhydrol.2016.10.032.

769

770 Hingray, B., Picouet, C., Musy, A. 2014. Hydrology: a science for engineers. Boca Raton,
771 USA: CRC Press.

772

773 Hrachowitz, M., Soulsby, C., Tetzlaff, D., Dawson, J.J.C., Dunn, S.M., and Malcolm,
774 I.A. 2009. Using long-term data sets to understand transit times in contrasting headwater
775 catchments. Journal of Hydrology, 367, 237 – 248.

776

777 Hugenschmidt, C., Ingwersen, J., Sangchan, W., Sukvanachaikul, Y., Duffner, A.,
778 Uhlenbrook, S., Streck, T. 2014. A three-component hydrograph separation based on

779 geochemical tracers in a tropical mountainous headwater catchment in northern Thailand.
780 Hydrol. Earth Syst. Sci., 18, 525-537.
781
782 Jafari SM, Zarre S, Alavipanah SK, Ghahremaninejad F. 2015. Functional turnover from
783 lowland to montane forests: evidence from the Hyrcanian forest in northern Iran. iForest
784 doi: 10.3832/ifor1002-008.
785
786 Libohova, Z., Schoeneberger, P., Bowling, L. C., Owens, P.R., Wysocki, D., Wills, S.,
787 Williams, C.O., Seybold, C. 2018. Soil Systems for Upscaling Saturated Hydraulic
788 Conductivity for Hydrological Modeling in the Critical Zone. Vadose Zone Journal, 17:
789 170051. Doi: 10.2136/vzj2017.03.0051.
790
791 Ma, Y., Li, X., L, Guo, L., Lin, H.S. 2017. Hydropedology: Interactions between
792 Pedologic and Hydrologic Processes across Spatiotemporal Scales. Earth-Science
793 Reviews 171:181-195.
794 Marengo, J. A., Alves, L.M. 2012. The 2011 intense rainfall and floods in Rio de
795 Janeiro. Bulletin of the American Meteorological Society 93: S176.

796 Menezes, M.D., Silva, S.H.G., Mello, C.R., Owens, P.R., Curi, N. 2014. Solum depth
797 spatial prediction comparing conventional with knowledge-based digital soil mapping
798 approaches. Scientia Agricola, 71, 316-323. DOI: 10.1590/0103-9016-2013-0416.
799

800 Monteith, J.I. 1964. Evaporation and environment, The State and Movement of Water in
801 Living Organisms. Proc. 19th Symp. Soc. Exp. Biol., Swansea, Academic Press, New
802 York (1964), pp. 205-234.
803
804 Mu, Q., Heinsch, F. A., Zhao, M., and Running, S. W. 2007. Development of a global
805 evapotranspiration algorithm based on MODIS and global meteorology data. Remote
806 Sensing of Environment, 111(4), 519-536.
807
808 Muñoz-Villers, L.E., Geissert, D. R., Holwerda, F., McDonnell, J. J. 2016. Factors
809 influencing stream baseflow transit times in tropical montane watersheds. Hydrology and
810 Earth System Science, 20, 1621-1635.
811
812 Muñoz-Villers, L.E. and McDonell, J.J. 2013. Land use change effects on runoff
813 generation in a humid tropical montane cloud forest region. Hydrology and Earth System
814 Science, 17, 3543–3560.
815
816 Muñoz-Villers, L.E., Holwerda, F., Gómez-Cárdenas, M., Equihua, M., Asbjornsen, H.,
817 Bruijnzeel, L.A., Marin-Castro, B.E., Tobón, C. 2012. Water balances of old-growth and
818 regenerating montane cloud forests in central Veracruz, Mexico. Journal of Hydrology,
819 462-463, 53-66 (DOI: 10.1016/j.jhydrol.2011.01.062).
820
821 Muñoz-Villers, L.E., Holwerda, F., Gómez-Cárdenas, M., Equihua, M., Asbjornsen, H.,
822 Bruijnzeel, L.A., Marin-Castro, B.E., Tobón, C. 2011. Water balances of old-growth and

regenerating montane cloud forests in central Veracruz, Mexico. Journal of Hydrology, 462-463, 53-66 (DOI: 10.1016/j.jhydrol.2011.01.062).

Oliveira, A.S., 2014. Recarga subterrânea de nascentes em ambientes distintos da região Alto Rio Grande, Universidade Federal de Lavras, Lavras, Brazil (Ph.D. Dissertation).

Oliveira Filho, A.T., Scolforo, J.R.S., Oliveira, A.D., Carvalho, L.M.T. 2006. Definição e delimitação de domínios e subdomínios das paisagens naturais do estado de Minas Gerais. In: J.R.S Scolforo, LMT Carvalho, eds, Mapeamento e Inventário da Flora e dos Reflorestamentos de Minas Gerais. Lavras, MG: UFLA, 21-35.

ORNL DAAC. 2018. MODIS and VIIRS Land Products Global Sub-setting and Visualization Tool. ORNL DAAC, Oak Ridge, Tennessee, USA. Accessed July 04, 2018. Subset obtained for MOD16A2 product at 22.1S,44.45W, time period: 2001-01-01 to 2018-06-10, and subset size: 6.5 x 6.5 km. https://doi.org/10.3334/ORNLDAAC/1379.

Pereira, D.R., Mello, C.R., Silva, A.M., Yanagi, S.N.M. 2010. Evapotranspiration and estimation of aerodynamic and stomatal conductance in a fragment of Atlantic Forest in Mantiqueira Range Region, MG. Cerne, 16, 32-40.

Pinto, L.C., Mello, C.R., Owens, P.R., Norton, L.D., Curi, N. 2015. Role of Inceptisols in the Hydrology of Mountainous Catchments in Southeastern Brazil. Journal of Hydrologic Engineering. DOI: 10.1061/(ASCE)HE.1943-5584.0001275.

Running, S., Mu, Q. 2017. MOD16A2 MODIS/Terra Net Evapotranspiration 8-Day L4 Global 500m SIN Grid V006. NASA EOSDIS Land Processes DAAC. https://doi.org/10.5067/MODIS/MOD16A2.006

Salemi, L.F., Groppo, J.D., Trevisan, R., Moraes, J.M., Ferraz, S.F.B., Villani, J.P., Duarte-Neto, P.J., Martinelli, L.A. 2013. Land-use change in the Atlantic rainforest region: consequences for the hydrology of small catchments. Journal of Hydrology, 499, 100-109.

Scolforo, J.R.S., Rufini, A.L., Mello, J.M., Oliveira, A.D., Silva, C.P.C. 2008. Equações para quantidade de carbono das fisionomias, em Minas Gerais. In: Scolforo, J.R.S., Oliveira, A.D., Acerbi Júnior, F.W. (eds). Inventário Florestal de Minas Gerais: Equações de Volume, Peso de Matéria Seca e Carbono para diferentes Fitofisionomias da Flora Nativa. Lavras, MG: Editora Ufla, 197-215.

Shuttleworth, W.J., 1992. Evaporation. In: D.R. Maidment, (ed.) Handbook of Hydrology, chap.4, 53p.

Tabarelli M, Aguiar AV, Ribeiro MC, Metzger JP, Peres CA (2010) Prospects for biodiversity conservation in the Atlantic Forest: lessons from aging human-modified landscapes. Biological Conservation 143:2328–2340

868 Terra, M.C.N.S, Mello, C.R., Mello, J.M. et al. 2017. Stemflow in a neotropical forest
869 remnant: vegetative determinants, spatial distribution and correlation with soil moisture.
870 Trees, DOI 10.1007/s00468-017-1634-3.
871
872 Terra, M.C.N.S., Mello, J.M., Mello, C.R., Santos, R.M., Nunes, A.C.R., Raimundo,
873 M.R. 2015a Influência topo-edafo-climática na vegetação de um fragmento de Mata
874 Atlântica na Serra da Mantiqueira, MG. Revista Ambiente & Água, 10, 928-942.
875
876 Terra, M.C.N.S., Mello, J.M., Mello, C.R. 2015b. Relação Espacial do Carbono da
877 Vegetação e Matéria Orgânica do Solo na Serra da Mantiqueira. Revista Floresta e
878 Ambiente. http://dx.doi.org/10.1590/2179-8087.059713
879
880 Tomasella, J., Hodnett, M.G., Cuartas, L.A., Nobre, A.D., Waterloo, M.J., Oliveira, S.M.,
881 2008. The water balance of an Amazonian micro-catchment: the effect of interannual
882 variability of rainfall on hydrological behavior. Hydrological Processes, 22, 2133-2147.
883 doi: 10.1002/hyp.6813.
884
885 Yin, Y., Wu, S., Zheng, D., Yang, Q. 2008. Radiation calibration of FAO56 Penman-
886 Monteith model to estimate reference crop evapotranspiration in China. Agricultural
887 Water Management, 95, 77-84. DOI: 10.1016/j.agwat.2007.09.002.
888
889 Wiekenkamp, I., Huisman, J.A., Bogena, H.R., Lin, H.S., Vereecken, H. 2016. Spatial
890 and temporal occurrence of preferential flow in a forested headwater catchment. Journal
891 of Hydrology, 534, 139-149.

Zema, D.A., Lucas-Borja, M.E., Carrà, B.G., Denisi, P., Rodrigues, V.A., Ranzini, M., Arcova, F.C.S., Cicco, V., Zimbone, S.M. Simulating the hydrological response of a small tropical watershed (Mata Atlantica, Brazil) by the AnnAGNPS model. Science of the Total Environment, 636, 737-750.

Zimmermann, B., Zimmermann, A., Scheckenbach, H.L., Schmid, T., Hall, J.S., van Breugel, M. 2013. Changes in rainfall interception along a secondary forest succession gradient in lowland Panama. Hydrological and Earth Systems Science 17, 4659-4670.

List of Tables

Table 1. Daily gross precipitation (P), canopy rainfall interception (C), and evapotranspiration (ET) for AFMC according to the seasons of the studied hydrological years.

Hydrological Year	Season	P (mm d^{-1})	C (mm d^{-1}) (C/P, %)	ET (mm d^{-1})

2009 - 2010	Wet	10.24	2.14 (20.9)	4.84
	Dry	1.49	0.37 (24.8)	1.58
	Hydrological year	5.86	1.25 (21.3)	3.21
2010 - 2011	Wet	13.82	2.87 (20.8)	5.09
	Dry	0.80	0.13 (16.3)	1.53
	Hydrological year	7.31	1.50 (20.5)	3.31

910

911

912

913

914

915

916

917 Table 2. Streamflow, baseflow, and baseflow index (BFI) coefficient for seasons of the
918 studied hydrological years in AFMC.

Hydrological year	Season	Streamflow ($mm\ d^{-1}$)	Base flow ($mm\ d^{-1}$)	BFI
	Wet season	2.86	2.10	0.74

2009-2010	Dry season	1.31	1.10	0.84
	Hydrological year	2.09	1.60	0.77
2010-2011	Wet season	3.85	2.50	0.65
	Dry season	1.09	0.97	0.89
	Hydrological year	2.47	1.74	0.70

Table 3. Multiple regressions for baseflow and overland flow in the AFMC as a function of soil water storage (SWS) in different layers, evapotranspiration, and throughfall.

Hydrologic Variable	Explaining variables	Estimate parameter	*p*-value (*t*)	Ajusted-R^2
Streamflow (overland flow + baseflow)	(Intercept) Throughfall (mm)	5.73593 0.27284	0.7007 3.11e-05***	0.6197

	SWS 20-60 cm	0.31514	0.00622**	
Overland flow	(Intercept)	-10.63396	0.37755	0.7077
	Throughfall (mm)	0.24029	2.25e-06***	
	SWS 20-60 cm	0.62341	0.00435**	
	SWS 60-100 cm	-0.50479	0.04583*	
Baseflow	(Intercept)	-9.8888	0.457907	0.4803
	SWS 60-100 cm	0.19736	0.011014*	
	Evapotranspiration	0.34162	0.000433***	

Note: *p*-value (*t*) means *p*-value of the *t*-test applied to the parameter: * significant at 0.05; ** significant at 0.01; *** significant at 0.001.

Table 4. Variation in water storage in the entire AFMC (ΔAFMC), in unsaturated zone (ΔS_{soil}), and estimated potential groundwater recharge (GS, for the end of the wet seasons) in the studied hydrological years.

Hydrological year	Season	ΔAFMC (mm)	ΔS_{soil} (mm)	GS (mm)
2009-2010	Wet season	461.3	57.5	403.8
	Dry season	-258	-88	-
	Hydrological Year	203	-	-
2010-2011	Wet season	889.6	179.1	710.5
	Dry season	-335.1	-190	-
	Hydrological year	554.5	-	-

944

945

946

947

948

949

950

951

952 **Figure captions**

953 **Figure 1.** Geographical location and instrumentation used for monitoring water balance
954 elements in the AFMC, Mantiqueira Range, Minas Gerais (MG) state, southeastern
955 Brazil.

956

957 **Figure 2.** Average water table depth between 2009 and 2011 in an AFMC neighboring
958 micro-catchment also located in the Lavrinha Creek Watershed as observed by Oliveira
959 (2014) (see the piezometers' location in Fig. 1).

960

961 **Figure 3.** Monthly gross precipitation, throughfall and its standard errors as observed in
962 the AFMC during the hydrological years of 2009-2010 and 2010-2011 (a) and average
963 monthly gross precipitation and respective standard deviation as observed in the Lavrinha
964 Creek Watershed from 2006 to 2012 (b).

965

966 **Figure 4.** Relationship between evapotranspiration modeled (ET) and evapotranspiration
967 from water balance (ET_{WB}) during the dry periods in AFMC site (a), and comparison
968 between ET 8-day modeled and ET 8-day from MODIS (b, c).

969

970 **Figure 5.** Temporal behavior of the leaf area index (monthly) (a), evapotranspiration
971 (daily and monthly values) (b), air temperature (hourly, daily and monthly values) (c),
972 and net radiation (daily and monthly values) in the AFMC throughout the studied period
973 (2009 to 2011).

974

975 **Figure 6.** Soil Water Storage dynamics (average and upper and lower limits calculated
976 based on the 25 locations for soil moisture measurement – Figure 1) throughout the
977 hydrological years from 2009 to 2011.

978

979 **Figure 7.** Classes of rainfall intensity frequency (a) and daily streamflow, base flow and
980 rainfall (b) throughout the hydrological years in the AFMC.

981

982 **Figure 8**. Daily water balance variation, potential groundwater recharge and daily rainfall
983 in the AFMC during the hydrological years of 2009/2010 and 2010/2011.

984

985

986

987

988